JOURNAL OF APPLIED ELECTROCHEMISTRY 17 (1987) 779–788

Electrochemical behaviour of copper in aqueous solution containing potassium ethylxanthate

J. GOMEZ BECERRA, R. C. SALVAREZZA, A. J. ARVIA

Instituto de Investigaciones Fisicoquímicas Teóricas y Aplicadas (INIFTA), Casilla de correo 16, Sucursal 4, (1900) La Plata, Argentina*

Received 19 August 1986; revised 11 November 1986

The electrochemical behaviour of copper in aqueous potassium ethylxanthate (KEX) is studied by using potentiodynamic techniques at different sweep rates, complemented with SEM and EDAX. In NaCl solutions a cuprous xanthate film is formed at low potentials, the initial stage of this reaction being the electroadsorption of KEX on copper competing with the adsorption of chloride ions and water. At low surface coverages for electroadsorbed KEX the electrodissolution of copper is partially inhibited as compared to plain NaCl solutions. As the KEX monolayer is completed, a tri-dimensional cuprous xanthate film grows in the electrode surface. On subsequent increase of the applied potential a complex anodic layer is formed leading to copper passivity. Passivity breakdown promoted by either chloride ions or electro-oxidation of the organic film can be observed when the potential exceeds a certain critical value.

1. Introduction

Potassium ethylxanthate (KEX) is used as a flotation agent in the separation of sulphide metal-containing ores, such as Cu_2S, PbS, etc. [1, 2]. The strong specific adsorption of xanthate on mercury [3, 4] turns its surface hydrophobic through a film of product due to a reaction with oxygen and adsorbed xanthate [5–8]. These types of interactions were also studied for other metals and metal sulphides in an attempt to disentangle the mechanism of mineral flotation [2, 9–11] which presumably involves charge transfer reactions.

Xanthate can adsorb on a clean metal surface through the formation of metal xanthate or dixanthogen by an oxidation process involving electron transfer and, in the presence of oxidation products, the adsorption of xanthate can occur by an ion-exchange reaction [12]. Nevertheless, from the experimental data available at present the electrochemical mechanism of flotation can not be unambiguously established [12–14].

The electrochemical reactions related to mineral flotation are, to some extent, directly comparable to those associated with corrosion, corrosion inhibition and metal passivity. Thus, mineral flotation involves at least a cathodic reaction, namely the electroreduction of molecular oxygen, and anodic processes concerning the electrooxidation of both metal and the surface active reagent. Therefore, the removal of dissolved oxygen eliminates the cathodic reaction, and the use of a clean metal surface should permit the study of the anodic process in relatively simpler conditions by means of conventional electrochemical techniques.

The present work was undertaken to investigate the behaviour of clean copper electrodes in different aqueous solutions containing KEX, in the absence of molecular oxygen, in an attempt to distinguish the occurrence of competitive electroadsorption processes, the electroformation of new phases and their electroreduction at interfaces exhibiting a great hydrophobicity.

2. Experimental details

Working electrodes were made of copper rods

* Facultad de Ciencias Exactas, Universidad Nacional de La Plata.

0021–891X/87 $03.00 + .12

axially embedded in Araldite holders to offer a flat disc-shaped area of 0.077 cm^2. The electrodes were successively polished with fine-grained emery paper and alumina paste of 1 μm, rinsed with acetone, and finally with twice-distilled water. A rotating disc electrode of exposed area 0.125 cm^2 with the same pretreatment as described above was also used. The potential of the working electrode was measured against a saturated calomel electrode (SCE) which was connected to the cell through a Luggin–Haber capillary tip. The counter electrode was a large platinum plate placed in a separate compartment.

Experiments were performed in a conventional cell at 25° C. The following solutions were used: x M NaCl + y M KEX ($0.1 \leqq x \leqq 4$; $10^{-6} \leqq y \leqq 10^{-2}$); 0.1 M $Na_2B_4O_7$ (pH 9.0) + 0.2 M NaCl + y M KEX. Solutions were prepared from twice-distilled water and Analar chemicals, and deareated by bubbling purified nitrogen for 3 h prior to the electrochemical measurements.

Single (STPS) and repetitive triangular potential sweeps (RTPS) were applied to the working electrode at different scan rates (v), where $0.01\,V\,s^{-1} < v < 0.1\,V\,s^{-1}$. Breakdown potentials ($E_b$) were measured through the potentiodynamic technique at $v = 0.001\,V\,s^{-1}$. SEM micrographs of the films formed during the polarization of the electrode were pictured with a Philips 500 scanning electron microscope with an EDAX system.

3. Results

3.1. *Current–potential characteristics for copper in 0.1 M NaCl*

The apparent current density (j) versus potential (E) profiles for copper in 0.1 M NaCl, run between $E_{s,c} = -0.50$ V and $E_{s,a} = 0.0$ V at $1\,mV\,s^{-1}$, show that the current changes from cathodic to anodic at ~ -0.20 V. At potentials greater than -0.1 V the anodic current increases rather abruptly due to the active dissolution of copper (Fig. 1). Otherwise, the j–E profile run at $0.1\,V\,s^{-1}$ from $E_{s,c} = -1.20$ V to $E_{s,a} = 0.0$ V shows a small peak (Ia) at ~ -0.56 V and an increase in anodic current at -0.37 V which presumably corresponds to a very small peak

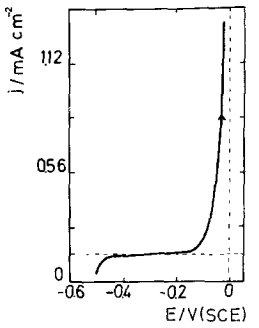

Fig. 1. j–E profile for copper recorded in 0.1 M NaCl at 25° C and $0.001\,V\,s^{-1}$ between $E_{s,c} = -0.50$ V and $E_{s,a} = -0.0$ V; $\omega = 0$ r.p.m.

(I′a) preceding the active dissolution region (IIa). The reverse scan exhibits a cathodic peak (IIc) at ~ -0.25 V and two small plateaux (I′c and Ic) at -0.50 and -0.91 V, respectively (Fig. 2), and a rather rapid increase in the cathodic current beyond -1.0 V. Voltammetric runs from $E_{s,c} = -1.20$ V to $E_{s,a}$ increased stepwise along the successive potential cycles reveal that each pair of contributions, Ia/Ic and I′a/I′c, is associated with one particular redox system at the copper surface level, whereas the electroreduction of soluble copper species produced in the active dissolution region (IIa) occurs within the potential range of current peak IIc. The electrode rotation decreases the height of peak IIc without changing the peak ratios Ia/Ic and

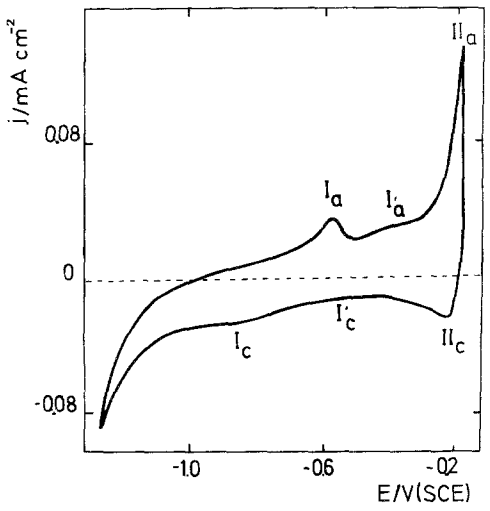

Fig. 2. STPS for copper recorded in 0.1 M NaCl at 25° C and $0.1\,V\,s^{-1}$ between $E_{s,c} = -1.20$ V and $E_{s,a} = -0.20$ V; $\omega = 1000$ r.p.m.

I'a/I'c. The increase in NaCl concentration shifts the potentials of peaks Ia, I'a, Ic and I'c to more negative values without any appreciable change in the corresponding voltammetric charge. As previously observed on silver [15] the pair of contributions Ia/Ic and I'a/I'c are related to the electroformation and electroreduction of either CuCl or $(CuCl)_2^-$ at the submonolayer level on copper. The corresponding charges are estimated as $q_{Ia} = 80\,\mu C\,m^{-2}$ and $q_{I'a} = 30\,\mu C\,m^{-2}$, respectively. At potentials more positive than -0.2 V the electrodissolution of copper yields both $CuCl_2^-$ complexes and CuCl(s).

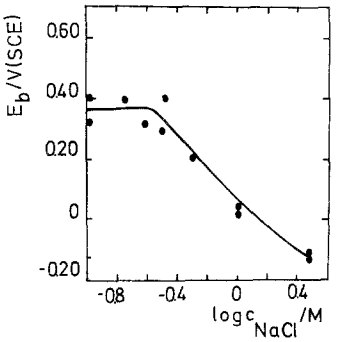

Fig. 4. Plot of E_b versus log c_{NaCl} at 25°C, 0.001 V s^{-1}, $c_{KEX} = 1 \times 10^{-3}$ M, $\omega = 0$ r.p.m.

3.2. *Current–potential characteristics of copper in NaCl solutions containing KEX*

The j–E profiles of copper in 0.1 M NaCl + y M KEX ($10^{-4} < y < 2 \times 10^{-3}$) run at $v = 0.001$ V s^{-1} from $E_{s,c} = -0.50$ V upwards change according to the concentration of KEX in the solution (Fig. 3a). For $c_{KEX} = 1 \times 10^{-4}$ M, the active dissolution starts rather abruptly as the potential exceeds -0.1 V. Furthermore, the threshold potential for copper electrodissolution moves progressively to more positive values and a more extended passive region can be observed as the concentration of KEX increases. On the other hand, for $c_{KEX} > 5 \times 10^{-4}$ M an anodic current hump in the -0.20 to -0.05 V range is noticed. This hump is followed by a small anodic peak preceding an abrupt current jump associated with pitting corrosion of copper when the potential exceeds a certain critical value (E_b). These results reveal

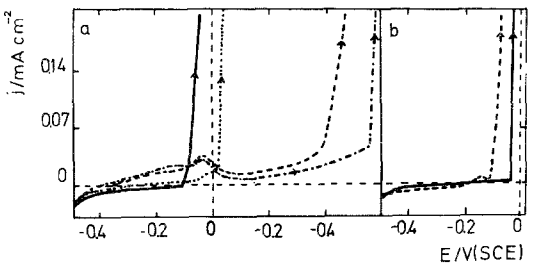

Fig. 3. (a) j–E profiles for copper recorded in 0.1 M NaCl at different c_{KEX} at $v = 0.001$ V s^{-1} started from $E_{s,c} = -0.50$ V; $\omega = 0$ r.p.m. c_{KEX}: 10^{-4} M (——); 5×10^{-4} M (···); 2×10^{-3} M (– – –); 3×10^{-3} M (–·–). (b) j–E profiles for copper recorded in 0.1 M NaCl at different values of c_{BTA} at $v = 0.001$ V s^{-1}, started from $E_{s,c} = -0.50$ V, $\omega = 0$ r.p.m: $c_{BTA} = 10^{-3}$ M (– – –); 3×10^{-3} M (——).

protective characteristics of the passive layer formed on copper in the presence of KEX. For comparison, similar runs were made in 0.1 M NaCl containing a well-known corrosion inhibitor for copper such as benzotriazol (BTA) (Fig. 3b). It can be seen that for comparable concentrations, the potential value associated with copper dissolution for BTA is nearly 0.6 V lower than that for KEX.

The increase in c_{NaCl} from 0.5 to 4 M for a constant c_{KEX} shifts E_b in the negative direction according to a linear E_b versus log c_{NaCl} dependence, but the value of E_b remains practically constant for NaCl concentrations lower than 0.5 M (Fig. 4). The increase in ω shifts E_b towards more positive potentials and also decreases the current in the passive region.

The effect of the immersion time of copper into the KEX-containing solutions was studied by holding the electrode at -0.50 V for different times (10 s $< t_a <$ 900 s) before running the j–E profiles at $v = 0.001$ V s^{-1}. The coincidence of j–E profiles resulting for different t_a suggests a relatively fast adsorption interaction between the copper and KEX.

Voltammograms for copper in 1.0 M NaCl + 1×10^{-3} M KEX at $v = 0.1$ V s^{-1} and $\omega = 1000$ r.p.m. run from $E_{s,c} = -1.70$ V to $E_{s,a} = 0.25$ V (Fig. 5) exhibit anodic peaks at -0.65 V (IIIa) and -0.50 V (IVa), the latter followed by an anodic limiting current (Va) in the -0.40 to -0.05 V range preceding the pitting corrosion range (IIa). A shoulder (VIa) appears at the initial portion of the electrodissolution process which is related to the anodic peak detected in the same potential range for j–E profiles at low

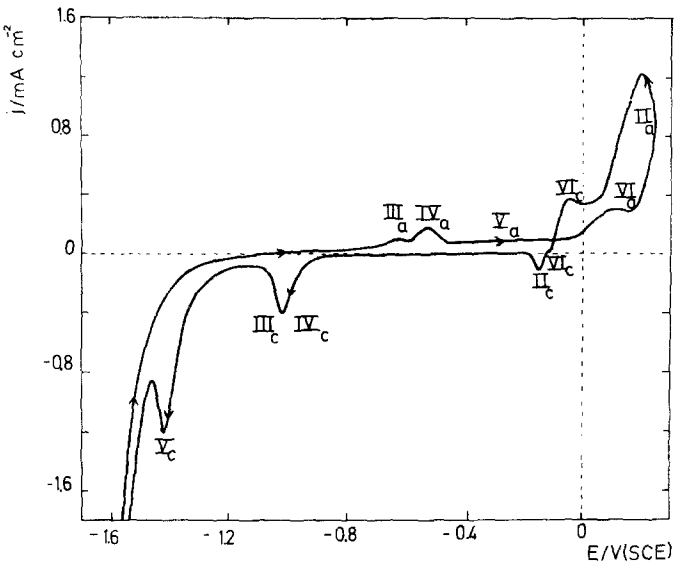

Fig. 5. STPS for copper recorded in 1 M NaCl + 1×10^{-3} M KEX at 25° C and 0.1 V s^{-1} between $E_{s,c} = -1.70$ V and $E_{s,a} = 0.25$ V; $\omega = 1000$ r.p.m.

sweep rates (Fig. 3a). The reverse scan shows a relative increase in current due to pitting corrosion of copper, a broad cathodic peak (IIc) at -0.20 V preceded by a hump (VIc), another broad complex cathodic peak (IIIc–IVc) at -1.080 V, and a sharp cathodic peak (Vc) at -1.450 V overlapping the hydrogen evolution current. Runs made from $E_{s,c} = -1.70$ V to values of $E_{s,a}$ increased stepwise show that peaks IIIa and IVa are related to current peaks IIIc–IVc (Fig. 6). The double-peak structure of peak IIIc–IVc can be resolved for low concentrations of KEX. From these runs one concludes that products formed in the potential range of Va are associated with the electroreduction process taking place in the potential range of peak Vc, whereas the products formed in the potential

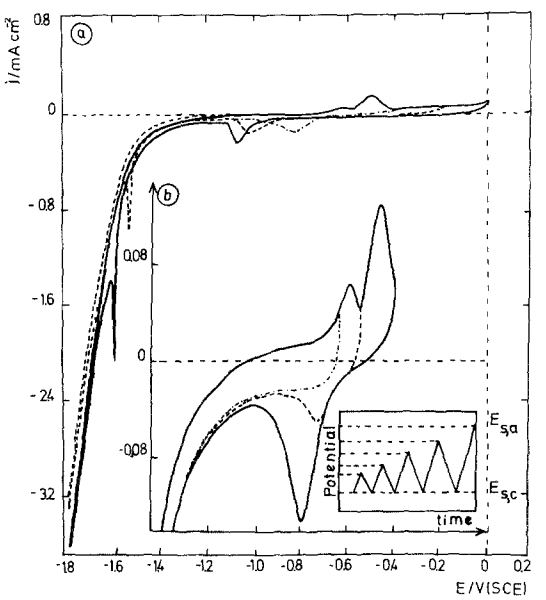

Fig. 6. (a) RTPS for copper recorded in 0.1 M NaCl + 1×10^{-3} M KEX at 25° C and 0.1 V s^{-1} between $E_{s,c} = -1.70$ V and $E_{s,a}$ charged stepwise in the positive direction; $\omega = 1000$ r.p.m. (b) Detail of the RTPS showed in Fig. 6a.

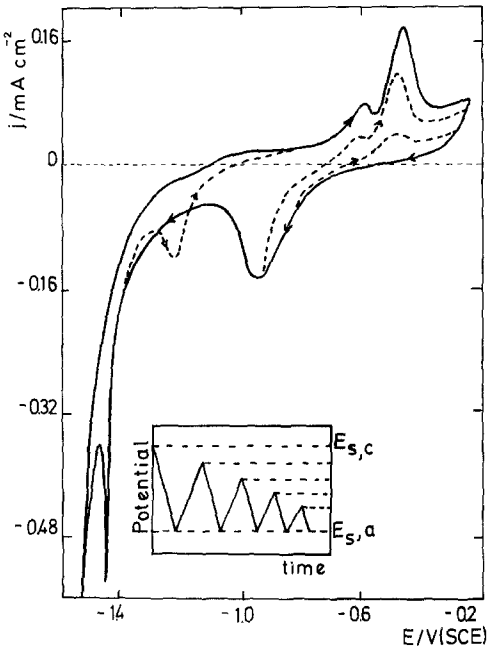

Fig. 7. RTPS for copper recorded in 0.1 M NaCl + 1×10^{-3} M KEX at 25° C and 0.1 V s^{-1} between $E_{s,a} = -0.25$ V and $E_{s,c}$ charged stepwise in the negative direction; $\omega = 1000$ r.p.m.

range IIa are electroreduced in the potential range of peak IIc.

Voltammograms recorded at $0.1\,V\,s^{-1}$ for $E_{s,a} = 0.25\,V$ and $E_{s,c}$ increased stepwise within a potential range more positive than those of peaks IIIc–IVc (Fig. 7) show a gradual increasing passivity of copper presumably caused by the formation of a surface layer. Passivity is gradually removed as $E_{s,c}$ is set at potentials more negative than that corresponding to the initiation of peak IVc. For $E_{s,c} = -1.40\,V$ the electroreduction scan exhibits only current peaks IIIc and IVc, whereas peak Vc is shown in the positive scan at 0.10 V more positive than that observed when $E_{s,c} = -1.70\,V$. This suggests that the electroreduction process related to peak Vc depends on the time the electrode is held in the potential region of the hydrogen evolution region (HER). RTPS runs from -0.25 to $-1.050\,V$ (Fig. 8) show a decrease in the heights of peaks IIIa, IVa, IIIc and IVc as compared to the first scan, and the potential of peak IVc moves in the positive direction. However, after 5 min RTPS the change of $E_{s,c}$ from -1.050 to $-1.70\,V$ reveals a large hysteresis in the voltammogram between -1.5 and $-1.1\,V$, and peak Vc appears as a complex and relatively large peak at $\sim -1.4\,V$. The subsequent anodic scan manifests a large increase in current which is presumably due to an increase in the electrode area. Therefore, as a consequence of the electroreduction process, passivity disappears and the electrodeposition of soluble copper species takes place in the HER potential range.

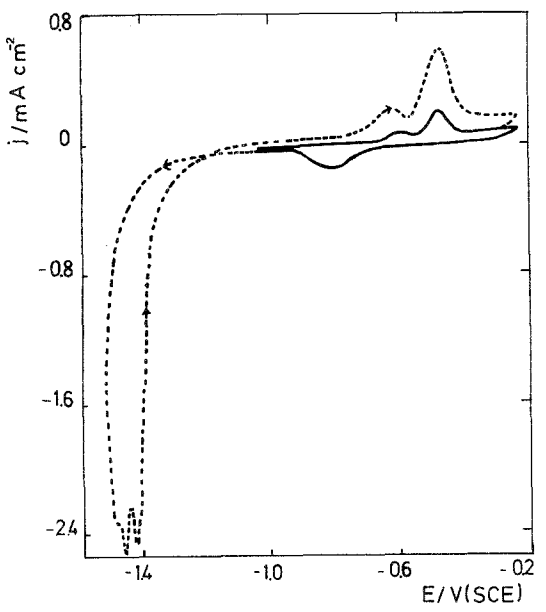

Fig. 8. j–E profile for copper recorded in 0.1 M NaCl + 1×10^{-3} M KEX at 25°C and $0.1\,V\,s^{-1}$ after RTPS for 5 min between $E_{s,c} = -1.0\,V$ and $E_{s,a} = 0.25\,V$ (——). Subsequent scan with $E_{s,c} = -1.6\,V$ (– – –). ω = 1000 r.p.m.

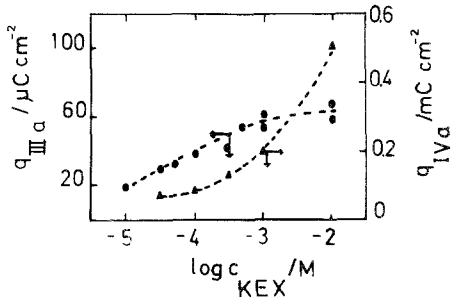

Fig. 9. Plots of q_{IIIa} versus log c_{KEX} (●) and q_{IVa} versus log c_{KEX} (▲) at 25°C. $c_{NaCl} = 0.1$ M; $v = 0.1\,V\,s^{-1}$; ω = 1000 r.p.m.

An increase in ω produces an increase in the current associated with peak VIa and a decrease in the current contributions IIa and IIc, while peaks IIIa, IVa, IIIc–IVc and Va remain practically unchanged.

The charge density (q) related to peak IIIa increases according to the concentration of KEX up to 1×10^{-3} M, but when the latter exceeds 10^{-3} M it remains practically constant ($q_{IIIa} \simeq 50\,\mu C\,cm^{-2}$) (Fig. 9). Conversely, q_{IVa} increases continuously with the concentration of KEX reaching, for 10^{-2} M, the value of $500\,\mu C\,cm^{-2}$. In addition, as the concentration of KEX increases, the peak potentials E_{IIIa}, E_{IVa} and E_{Va} shift in the negative direction and the corrosion region (IIa) moves towards more positive potentials. Both E_{IIIa} and E_{IVa} change linearly with log c_{KEX} and the corresponding slopes are 0.06 and 0.1 V per decade, respectively. As the concentration of NaCl changes from 0.1 to 1 M, a small decrease in the height of peaks IIIa and IVa is observed, and simultaneously peak Vc moves in the positive direction (Fig. 10).

The increase in pH moves the corrosion region (IIa) in the positive potential direction, turns shoulder VIa into a well-defined peak, originates a broad peak within the potential range of peak Va, and manifests a cathodic

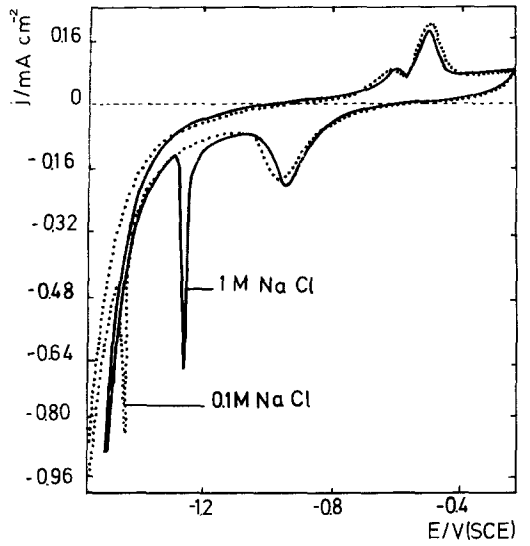

Fig. 10. STPS for copper recorded in x M NaCl + 1 × 10^{-3} M KEX at 25° C and V s^{-1} between $E_{s,c} = -1.70$ V and $E_{s,a} = 0.25$ V. Values of x: 0.1 M (···); 1 M (——). $\omega = 1000$ r.p.m.

contribution at ~ −0.70 V. The last two current contributions can be related to copper oxide electroformation and electroreduction, respectively. It should be noticed, however, that at pH 11, for instance, the corresponding electroreduction charge becomes smaller than that observed for plain 0.1 M NaCl.

Complementary voltammetric runs made with copper electrodes which had been previously heated in air show that thermally formed copper oxides can be electroreduced in the potential range where peak Vc (Fig. 11) is observed. Therefore, it is likely that peak Vc is to a great extent related to the electroreduction of a poorly hydrous copper oxide.

The influence of KEX on the formation of copper oxides was also studied in borate–boric acid containing 0.2 M NaCl + y M KEX ($10^{-6} < y < 10^{-2}$) through voltammetric runs at 0.001 V s^{-1} starting from −1.00 V up to E_b (Fig. 12). In the absence of KEX, anodic peaks at −0.20, 0.0 and ~0.3 V can be observed. In this case the value of E_b lies at ~0.75 V. The first peak can be associated with Cu_2O electroformation, and the remaining peaks correspond to an electro-oxidation yielding either CuO or $Cu(OH)_2$. The presence of small amounts of KEX (less than 5×10^{-4} M) produces a large increase in current in the potential range where the electroformation of Cu_2O takes place. This suggests that in the presence of KEX the passive properties of the anodic layer are diminished and the attack of copper by chloride ions becomes more likely. Correspondingly, the peak potentials move towards more positive values and, finally, the passivity of copper can be restored in the 0.4 V to E_b range. Likewise, as the concentration of KEX increases, E_b shifts slightly towards more positive potentials. On the other hand, for concentrations of KEX greater than 5×10^{-4} M the current in the entire region related to oxide electroformation decreases according to the concentration of

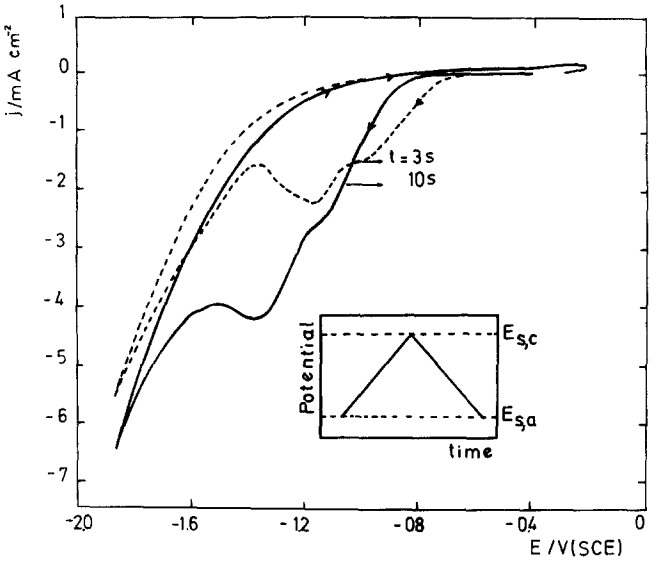

Fig. 11. STPS for copper recorded in 0.1 M NaCl at 25° C and 0.1 V s^{-1} between $E_{s,a} = 0.20$ V and $E_{s,c} = -1.85$ V for a copper wire heated in air for 3 s (– – –) or 10 s (——).

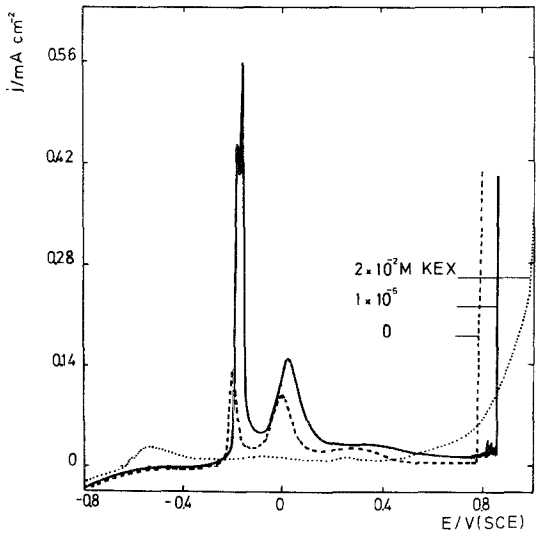

Fig. 12. j–E profiles for copper recorded in borax buffer + 0.2 M NaCl + c_{KEX} at 25° C and 0.001 V s^{-1} from $E_{s,c}$ = −0.80 V to E_b. c_{KEX}: 0 (---); 1 × 10^{-5} M (——); 1 × 10^{-2} M (···).

KEX. Simultaneously, a small anodic current is observed at potentials more negative than −0.4 V. Finally, for 10^{-3} M < c_{KEX} < 10^{-2} M, two anodic peaks, one at −0.63 V and another at −0.55 V, are observed, whereas the peaks associated with the oxide formation become broad and poorly defined at potentials more positive than those observed at lower concentrations of KEX. In this case a relatively large anodic current in the potential region preceding E_b is recorded and, simultaneously, a yellow product spills away from the electrode surface into the cell. The current peaks observed at −0.63 and −0.55 V are related to the electroformation of Cu–KEX layers, as detected in plain solution containing NaCl + KEX. The electro-oxidation of these layers occurs simultaneously with copper corrosion from 0.4 V upwards yielding Cu(II) xanthate and, probably, a certain amount of dixanthogen from the electro-oxidation of xanthate ion on the copper surface [9].

3.3. *SEM observations and EDAX data*

SEM observations were carried out on copper electrodes previously electroreduced at −1.70 V in 0.1 M NaCl + 10^{-3} M KEX for 90 s and later held at a constant potential (E_s) covering the potential range of peak IVa, region Va and region IIa, for the time t_s. For $E_s = E_{IVa}$ and t_s = 30 min, a crystalline and porous film is

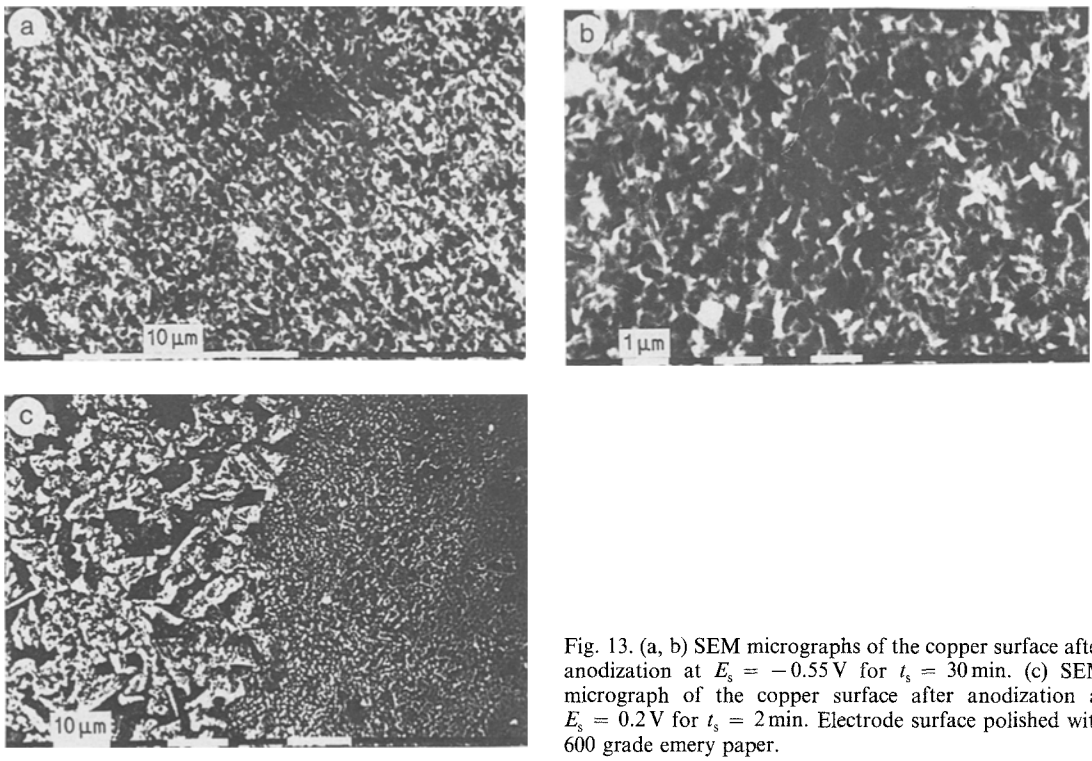

Fig. 13. (a, b) SEM micrographs of the copper surface after anodization at E_s = −0.55 V for t_s = 30 min. (c) SEM micrograph of the copper surface after anodization at E_s = 0.2 V for t_s = 2 min. Electrode surface polished with 600 grade emery paper.

formed on the copper surface (Fig. 13a, b) whose EDAX spectrum shows strong copper and sulphur signals. These results correspond to the Cu–KEX film. The same film is apparently also present for E_s set in the potential region Va, although in this case, for $t_s = 30$ min, the sulphur signal decreases. By setting E_s within region IIa, the film reveals a non-homogeneous island structure made of large crystals (Fig. 13c). At islands, EDAX data indicate strong copper and chloride signals, whereas the remaining electrode area shows only a small sulphur signal, presumably associated with a residual Cu–KEX film.

4. Discussion

The first stage of copper electrodissolution in NaCl-containing solutions involves the electroformation of a submonolayer of adsorbed chloride ions in the -0.55 to -0.30 V range preceding the active dissolution reaction [15]. These processes, however, are substantially changed when KEX is present in the solution. The present results confirm that the interaction of KEX molecules with copper, yielding a protective layer at low potentials, is comparable to the interaction of other molecules acting as inhibitors for copper corrosion. The adsorption of KEX on copper resembles that of benzotriazol, imidozole and mercaptobenzimidazole, which are adsorbed on copper in the -0.70 to -0.10 V range. In these cases the adsorbed film is revealed by surface-enhanced Raman scattering (SERS) and a.c. impedance measurements [16]. In the presence of inhibitors either a partial or a complete displacement of chloride ions from the copper surface by the inhibitor can be observed depending whether weak or strong inhibitors, respectively, are considered [17].

The adsorption of KEX on solid surfaces is well known due to its use in mineral flotation [1, 2]. The reversible potential for Cu(I) xanthate formation ($E_r/10^{-3}$ M KEX) is -0.69 V (SCE) [18]; it is therefore reasonable to assign peaks IIIa, IVa, IIIc and IVc to the electroformation and electroreduction of Cu(I) xanthate. The mechanism of formation of Cu(I) xanthate layer can be derived from the dependence of q_{IIIa} on the concentration of KEX. It is clear that q_{IIIa} increases according to the concentration of KEX up to 10^{-3}M to reach 50 μC per apparent cm^2. This limiting apparent charge density value, which remains practically independent of the concentration of KEX, suggests that the electrochemical reaction occurs at either monolayer or submonolayer level, presumably through the electroadsorption of xanthate ion (X^-) on copper at the early stage. The corresponding electroadsorption–electrodesorption process behaves as a relatively reversible process, and the fact that $dE_{IIIa}/d \log c_{KEX} = 0.06$ V per decade is consistent with a single electron exchange per X^- ion in the overall reaction:

$$Cu(s) + X^- = (CuX)_{ad} + e \qquad (1)$$

On the basis of Reaction 1 and a X^- to copper radii ratio (r_{X^-}/r_{Cu}) of 4, the maximal apparent charge density expected for a compact monolayer of X^- is 50 μC cm^{-2}, a value which agrees with the experimental limiting value of q_{IIIa}. Likewise, the fast electroadsorption of KEX on copper is confirmed by the fact that no changes in the j–E profiles are observed on increasing the adsorption time at any preset potential. Nevertheless, for concentrations of KEX lower than 10^{-3} M, small and stable values of q_{IIIa} are attained which probably result from the occurrence of a competitive adsorption among Cl^- ion, water and X^- ion for copper sites. These processes can be formally represented according to the following reactions:

$$Cu + X^- = Cu(X)_{ad} + e \qquad (2)$$

$$Cu + Cl^- = Cu(Cl)_{ad} + e \qquad (3)$$

$$Cu + H_2O = Cu(H_2O)_{ad} \qquad (4)$$

$$Cu(H_2O)_{ad} = Cu(OH)_{ad} + H^+ + e \qquad (5)$$

As the electroadsorption of X^- ion behaves as a reversible process, it is likely that at low concentration of KEX the surface coverage by the X^- ion is lower than that required for a complete monolayer. Hence, the interaction between Cl^- ion and water with copper should be enhanced so that the electrodissolution of copper can be assisted through the reactions:

$$Cu(Cl)_{ad} + Cl^- = (CuCl)_2^- + e \qquad (6)$$

$$(CuCl)_2^- = CuCl_2^-(aq) \qquad (7)$$

As reactions 6 and 7 proceed, the passivity of copper is gradually removed. Similarly, in the borax buffer containing both NaCl and a low concentration of KEX, copper electrodissolution is also favoured through Reactions 6 and 7, as the coverage of the copper surface by water molecules which are required for the oxide layer electroformation (Reactions 4 and 5) is substantially diminished due to X^- ion adsorption. Otherwise, as the applied potential increases, this situation can be reversed because adsorbed xanthate can be displaced from the copper surface by water. Then, the passive oxide layer can be formed according to:

$$(CuX)_{ad} + H_2O = Cu(H_2O)_{ad} + X^- \quad (8)$$

$$Cu(H_2O)_{ad} = Cu(OH)_{ad} + H^+ + e \quad (9)$$

$$Cu(OH)_{ad} \rightarrow \text{oxide layer} \quad (10)$$

On the other hand, for concentrations of KEX greater than 10^{-3} M, a complete monolayer of xanthate can be formed. The structure of the adsorbed layer may involve an interaction between the polar group of the molecule and the copper surface, so that the hydrophobic hydrocarbon chain points out towards the solution side, completely preventing a direct interaction of copper with either water or Cl^- ions. This fact favours the growth of a porous crystalline Cu(I) xanthate layer on the copper surface (Fig. 13a, b). However, at potentials more positive than -0.40 V the formation of a Cu(II) xanthate film in pores of the Cu(I) xanthate layer becomes possible. The presence of peak VIa and the observation of a broad current peak within region Va on increasing the pH of the solution suggests that copper oxides, presumably with a very low content of water, can also be simultaneously formed with the copper–organic matrix layer leading to a non-homogeneous complex anodic film. At this stage the electroformation of copper xanthate can be written as follows:

$$CuX + X^- \rightarrow (CuX_2) + e \quad (11)$$

$$(CuX_2) \rightarrow Cu + CuX \quad (12)$$

According to the literature [1] cupric xanthate resulting from Reaction 11 is unstable and disproportionates as indicated by Reaction 12, yielding a fresh copper surface and Cu(I) xanthate at the solution side. The electroreduction of the oxide constituents in this complex layer due to the hydrophobicity of the electrode–solution interface is more difficult than in KEX-free solutions. Apparently, its electroreduction occurs simultaneously with the HER. The overall process results in a porous copper structure and, consequently, in an increase in the electrode area.

The stability of the complex passive film formed at potentials more positive than -0.4 V depends on the applied potential as well as the NaCl and KEX concentrations. Thus, at low NaCl concentration, E_b becomes practically independent of concentration. Conversely, the increase in NaCl concentration beyond 0.5 M, moves the potential of peak Vc more positive, and simultaneously E_b shifts in the negative direction shortening the passive domain (Fig. 4). These results can be explained with the aid of the j–E profiles recorded in borax buffer + NaCl solutions (Fig. 12). Thus, for borax buffer + 0.1 M NaCl, the pitting of copper occurs at potentials more positive than those observed for the plain NaCl solution and, for a concentration of KEX higher than 10^{-3} M, a clear anodic current associated with the electro-oxidation of the organic film is seen before E_b is reached. Besides, at potentials more positive than 0 V, certain contributions due to the electro-oxidation of xanthate ions from solution to dixanthogen [18, 19] also occur, according to:

$$2X^- \rightarrow X_2 + 2e \quad (13)$$

As the concentration of KEX increases at a constant low c_{NaCl}, the electro-oxidation of the organic species occurs at more negative potentials. In the borax buffer the metal passivity is mainly due to the presence of a copper oxide film. The passivity breakdown is controlled by the Cl^- ions and E_b becomes practically independent of c_{KEX}. Thus, two processes (electro-oxidation of the organic film and passivity breakdown) are clearly separated. Conversely, in plain chloride-containing solutions, passivity breakdown depends on the potential of organic species electro-oxidation and c_{NaCl}. At low c_{NaCl} the E_b value is fixed by the potential at which the electro-oxidation of xanthate species to

dixanthogen occurs, a value which obviously depends on c_{KEX} and not on c_{NaCl}. As c_{NaCl} increases, the breakdown of the passive film by chloride ions occurs at more negative potentials than that corresponding to the electro-oxidation of the organic species so that E_b becomes dependent on c_{NaCl}. The electro-oxidation process is then related to the oxidation of xanthate ions to dixanthogen and strong copper dissolution as Cu^{2+} on the copper surface. In this case Cu^{2+} ions react with xanthate in solution, resulting in non-adherent cupric xanthate formation. After breakdown the nucleation and growth of CuCl occurs, leading to localized base metal corrosion. The presence of CuCl islands on the electrode partially covered by the complex film suggests that localized corrosion is related to the nucleation and growth of a salt of an aggressive anion at the passive film surface [20] as has already been observed for other metals in various aggressive environments [21].

Acknowledgement

This work was financially supported by the Universidad Nacional de La Plata, the Consejo Nacional de Investigaciones Científicas y Técnicas and the Comisión de Investigaciones Científicas de la Provincia de Buenos Aires.

References

[1] M. J. Jones, (ed), 'Complex Sulphide Ores', The Institution of Mining and Metallurgy, London (1980).
[2] P. E. Richardson, S. Srinivasan and R. Woods, Proc. Intern. Symp. on Electrochemistry in Mineral and Metal Processing, Vol. 84-10, The Electrochemical Society, Pennington (1984).
[3] N. K. Adam, *Nature* **123** (1929) 413.
[4] E. Tscherneva and A. Gorodetskaya, *Zh. Fiz. Kim.* **13** (1939) 1117.
[5] S. G. Salamy and J. C. Nixon, *Aust. J. Chem.* **7** (1954) 146.
[6] A. Pomianowski, Proc. 2nd Int. Congr. Surface Activity, Vol. 3, London (1957) p. 332.
[7] *Idem, Rocz. Chem.* **41** (1967) 775.
[8] *Idem,* Proc. Intern. Symp. on Electrochemistry in Mineral and Metal Processing, Vol. 84-10, The Electrochemical Society, Pennington (1984) p. 3.
[9] R. Woods, *J. Phys. Chem.* **75** (1971) 354.
[10] S. Chander and R. W. Fuersteneau, *J. Electroanal. Chem.* **56** (1974) 217.
[11] O. Huynth Thi, M. Lamache and D. Bauer, *Electrochim. Acta* **26** (1981) 33.
[12] M. D. Pritzker and R. H. Yoon, Proc. Intern. Symp. on Electrochemistry in Mineral and Metal Processing, Vol. 84-10, The Electrochemical Society, Pennington (1984) p. 26.
[13] I. Plaksin, *Trans. Amer. Inst. Nim. Eng.* **214** (1959) 314.
[14] J. O'M. Bockris and K. C. Pillai, Proc. Intern. Symp. on Electrochemistry in Mineral and Metal Processing, Vol. 84-10, The Electrochemical Society, Pennington (1984) p. 112.
[15] M. F. L. de Mele, R. C. Salvarezza, D. V. Vasquez Moll, H. A. Videla and A. J. Arvia, *J. Electrochem. Soc.* **123** (1986) 746.
[16] D. Thierry and C. Leygraf, *ibid.* **132** (1985) 1009.
[17] M. Fleischmann, I. R. Hill, G. Mengoli, M. M. Musiani and J. Akharan, *Electrochim. Acta* **30** (1985) 879.
[18] M. Hepel and A. Pomianowski, *Int. J. Miner. Process* **4** (1977) 345.
[19] R. Wood, *Aust. J. Chem.* **25** (1972) 2329.
[20] M. R. G. de Chialvo, D. V. Vasquez Moll, R. C. Salvarezza and A. J. Arvia, *Electrochim. Acta* **30** (1985) 1501.
[21] R. C. Salvarezza, D. V. Vasquez Moll and A. J. Arvia, 36th Meeting of the International Society of Electrochemistry, Salamanca, Spain, Extended Abstracts (1985) p. 6020.